

Modeling of lead ions transport through a bulk liquid membrane

Amer D.Z. Albdiri^{a,*}, Ahmed A. Mohammed^b, Maad Hussein^b, Stanislaw Koter^c

^aChemical Engineering Department, University of Al-Qadisiyah, Ad Diwaniyah, 88, Iraq, email: amer_zmat@yahoo.com

^bEnvironmental Engineering Department, Baghdad University, Baghdad, 16714, Iraq, emails: ahmed.abedm@yahoo.com (A.A. Mohammed), altaaamaad@yahoo.com (M. Hussein)

^cFaculty of Chemistry, Nicolaus Copernicus University, Torun, ul, Gagarina 7, 87–100, Poland, email: skoter@umk.pl

Received 24 May 2019; Accepted 26 October 2019

ABSTRACT

The transport of lead ions (Pb^{2+}) through an organic liquid membrane (kerosene) containing (2.5%–12.5% v/v) Tri-n-butyl phosphate (TBP) as a carrier, under various operating conditions were experimentally investigated and modeled. The effect of the strip to feed volume ratio ($V_s:V_f$), variable membrane volume, and wide range of feed and strip pH on the transport of lead ions (Pb^{2+}) were modeled using a simple kinetic model and experimentally validated. The diffusion boundary layer and steady-state conditions were assumed for the solution of the transport model. The Pb^{2+} ions time-dependent concentrations within feed, membrane, and strip phases were found to be fairly comparable to experimental results. Probable leakage (bleeding between feed and strip phases) and non-leakage conditions were considered in the model. Results have shown that the transport rate is a strong function of pH and partition coefficient. It was also concluded that working at higher $V_s:V_f$ favors the transport of Pb^{2+} and higher removal efficiencies were obtained.

Keywords: Bulk liquid membrane; Lead permeation; Diffusion boundary layer

1. Introduction

Lead has been reported to be a cumulative poisonous heavy metal and widely found in the environment [1]. Mining, smelting, fuel additive, and battery manufacturing industries are considered as a major source of lead pollution [2,3]. The removal of lead from industrial wastewaters becomes a challenge to researchers, and many attempts to extract lead from aqueous solutions were reported [4–9].

Liquid membranes technique has emerged as a competitive separation process for the extraction of heavy metals from industrial wastewaters [10,11]. Liquid membrane process usually utilizes an extracting reagent solution, immiscible with water, stagnant between two aqueous solutions, the source or (feed) and receiving or (strip) phases [12].

Mathematical modeling of liquid membrane processes has been considered by many researchers [13–15] to describe

the transport of solutes through liquid membranes and to predict the performance of the separation (pertraction) processes. Models based on consecutive reversible or irreversible first-order reactions were frequently reported [16,17] showing fluctuations between poor to fair agreement with experimental data. However, Koter et al. [18] succeeded in model cadmium transport through a bulk liquid membrane containing D2EHPA as a carrier using Nernst–Planck equation and demonstrated a satisfactory agreement between model and experimental results. Unfortunately, to the knowledge of the authors, the modeling of the transport of the lead ions through the liquid membrane has not yet received considerable attention. Mohammadi et al. [20] attempted the modeling of metal ions transport through supported liquid membrane using the dimensionless model for the determination of the mass transfer coefficient. Sadyrbaeva [21] reported that using electrodialysis through bulk liquid membrane enhances the extraction and deposition of lead(II) from aqueous acidic

* Corresponding author.

solutions. Durmaz et al. [22] demonstrated the successful use of a multi-dropped liquid membrane system to transport lead ions under a diffusion-controlled process. El-Said et al. [23] suggested a simple pertraction permeable model using the transport of lead(II) controlled by a membrane diffusion mechanism. Arous et al. [24] used cellulose triacetate as a membrane to efficiently solve the enduring problem of membrane stability and concluded that transport through a polymer inclusion membrane was increased. Pei and Wang [25] used a disphase supplying supported liquid membrane (DSSLM) for the recovery of lead(II) from solutions, and a model of new kinetic equations was developed to describe the reaction and transport of lead ions in the DSSLM. However, it was found that most of the reported approaches to model the lead(II) transport were limited and specific to metal recovery.

In this work, a diffusive layers mechanism was adopted to model the permeation of lead from lead acetate aqueous solution (feed phase) to a basic solution (stripping phase) through two diffusion layers (feed-liquid membrane interface, and liquid membrane-stripping interface) and a bulk liquid membrane (kerosene) stagnant between the feed and stripping phases. The model satisfactorily described the experimental data.

2. Theory

The scheme of the modeled system is shown in Fig. 1. As shown, the bulk liquid membrane (kerosene and tri-n-butyl phosphate (TBP) as a carrier) separates feed-side and stripping-side diffusion layers. The Pb^{2+} ions slowly diffuse through the feed-side diffusion layer. Hence, it is considered the rate control step of the transport phenomena.

2.1. Feed phase ($Pb(CH_3COO)_2$ solution + HCl)

Burns and Hume [19] demonstrated that lead acetate solution dissociates into Pb^{2+} , PbA^+ , PbA_2 , PbA_3^- , where A denotes CH_3COO^- . The formation constants of the three acetate complexes (PbA^+ , PbA_2 , PbA_3^-) were reported by Burns and Hume [19]; $K_{f,1} = 145$, $K_{f,2} = 810$, $K_{f,3} = 2,950$ respectively. The dissociation of $Pb(CH_3COO)_2$ is expressed in Eq. (1).

$$K_{f,i} = \frac{[PbA_i^{2-i}]}{[Pb^{2+}][A^-]^i} \quad i = 1, 2, 3 \quad (1)$$

$$C_{Pb(II)} = [Pb^{2+}] + [PbA^+] + [PbA_2] + [PbA_3^-] \quad (2)$$

$$C_A = [A^-] + [PbA^+] + 2[PbA_2] + 3[PbA_3^-] + [HA] \quad (3)$$

For the initial solution; the equality $2C_{Pb(II)} = C_A$ holds, and Eqs. (1) and (2) result in Eq. (4).

$$[PbA_i^{2-i}] = \frac{C_{Pb(II)}[A^-]^i K_{f,i}}{1 + \sum_{j=1}^3 [A^-]^j K_{f,j}} \quad i = 0, 1, 2, 3 \quad (4)$$

where for $i = 0$, $K_{f,0} = 1$. Substituting [HA] from Eq. (3) into the formula for dissociation constant of HA:

$$K_a = \frac{[H^+][A^-]}{[HA]} \quad (5)$$

Eq. (5) can be solved with respect to $[A^-]$ for a given pH. Then $[Cl^-]$ can be determined from the electroneutrality condition for that solution:

$$2[Pb^{2+}] + [PbA^+] + [H^+] = [A^-] + [PbA_3^-] + [Cl^-] \quad (6)$$

Since pH is less than 7, $[OH^-]$ is neglected.

Therefore, only Pb^{2+} ions practically exist in the feed; $[Pb^{2+}]/C_{Pb(II)} > 0.99999$.

2.2. Strip phase (distilled water + 0.2 N NaOH solution + ethylenediaminetetraacetic acid as stripping agent)

$Pb(II)$ and ethylenediaminetetraacetic acid (EDTA) form a strong complex:

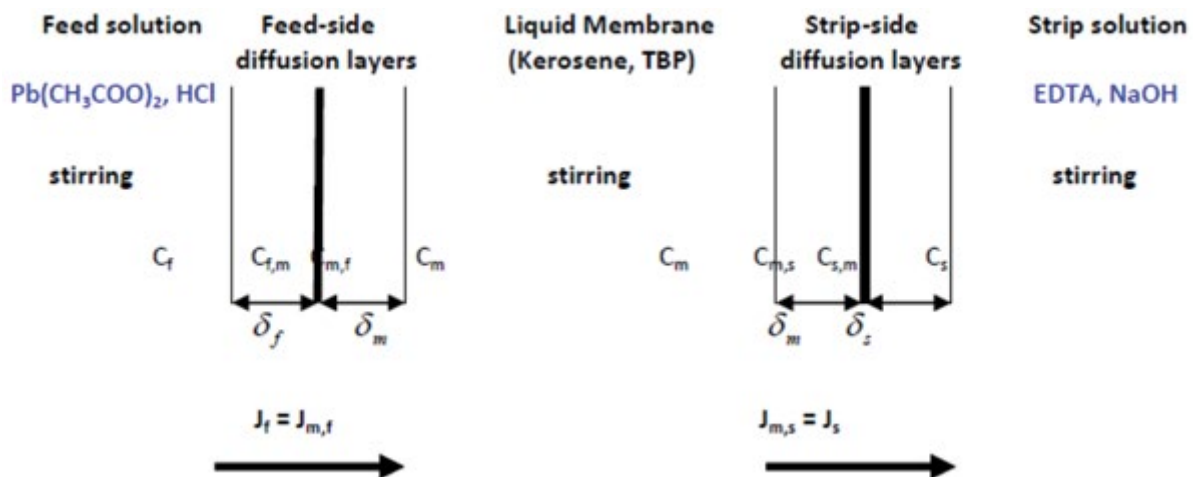


Fig. 1. Schematic representation of lead transport through the bulk liquid membrane.

The formation constant was reported to be 2×10^{18} [25], and because practically $\text{CEDTA} \gg C_{\text{Pb}^{2+}}$, only PbEDTA^{2-} exists in the strip phase. Also, Pb(OH)_2 is expected not to precipitate as ($K_{\text{sp}} = 1.42 \times 10^{-20}$) [26].

2.3. Transport model

Following the procedure in [19], the following assumptions hold (1) steady-state for diffusion layers and (2) fast equilibrium on both membrane boundaries (feed-membrane and membrane-strip).

For the feed-liquid membrane boundary layer, the following equations hold:

$$J_{\text{Pb},f} = \frac{D_f}{\delta_f} (C_f - C_{f,m}) = \frac{D_{m,f}}{\delta_{m,f}} (C_{m,f} - C_m) \quad (8)$$

$$K_{p,f} = \frac{C_{m,f}}{C_{f,m}} \quad (9)$$

where $J_{\text{Pb},f}$ is the Pb flux at the feed-membrane boundary, D is the resultant diffusion coefficient of Pb, δ_f , $\delta_{m,f}$ is the thickness of diffusion layers for feed and membrane sides respectively, $K_{p,f}$ is the partition (distribution) coefficient of Pb in the feed phase, C_f , C_m is the Pb concentration in the feed and membrane phases respectively, $C_{f,m}$, $C_{m,f}$ are the Pb concentration at the membrane surface of feed and membrane sides respectively. Eliminating $C_{m,f}$ and $C_{f,m}$ from Eqs. (8) and (9), the following expression for $J_{\text{Pb},f}$ is obtained:

$$J_{\text{Pb},f} = P_f (K_{p,f} C_f - C_m) \quad (10)$$

where:

$$P_f = \frac{\left(\frac{D_f}{\delta_f}\right) \left(\frac{D_{m,f}}{\delta_{m,f}}\right)}{\frac{D_f}{\delta_f} + \frac{K_{p,f} D_{m,f}}{\delta_{m,f}}} \quad (11)$$

Regarding the strip solution; the condition $C_{\text{EDTA}} > C_{\text{Pb}}$ holds and only $[\text{Pb(EDTA)}^{2-}]$ exists. Therefore:

$$J_{\text{Pb},s} = \frac{D_{m,s}}{\delta_{m,s}} (C_m - C_{m,s}) = \frac{D_s}{\delta_s} C_{s,m} \quad (12)$$

$$K_{p,s} = \frac{C_{m,s}}{C_{s,m}} \quad (13)$$

where $J_{\text{Pb},s}$ is the Pb flux at the strip-membrane boundary, D is the resultant diffusion coefficient of Pb, δ_s , $\delta_{m,s}$ are the thickness of diffusion layers for strip and membrane sides respectively, $K_{p,s}$ is the partition (distribution) coefficient of Pb in the strip phase, C_s , C_m are the Pb concentration in the strip and membrane phases respectively, $C_{s,m}$, $C_{m,s}$ are the Pb concentration at the membrane surface of strip and membrane sides respectively. Eliminating $C_{m,s}$ and $C_{s,m}$

from Eqs. (12) and (13), the following expression for $J_{\text{Pb},s}$ is obtained:

$$J_{\text{Pb},s} = P_s C_m \quad (14)$$

where:

$$P_s = \frac{\left(\frac{D_s}{\delta_s}\right) \left(\frac{D_{m,s}}{\delta_{m,s}}\right)}{\frac{D_s}{\delta_s} + \frac{K_{p,s} D_{m,s}}{\delta_{m,s}}} \quad (15)$$

The mass balance can be represented by the following differential equations:

$$\frac{dC_f}{dt} = -\frac{A_f}{V_f} J_{\text{Pb},f} = -k_{1f} C_f + k_{1b} C_m \quad (16a)$$

$$\frac{dC_s}{dt} = \frac{A_s}{V_s} J_{\text{Pb},s} = k_2 C_m \quad (16b)$$

where V_f , V_s are volumes of feed and strip solutions respectively, A_f , A_s are contact areas of feed-membrane and strip-membrane respectively. k_{1f} , k_{1b} , k_2 are related to the model parameters by the following equations:

$$k_{1f} = \frac{A_f}{V_f} K_{p,f} P_f \quad (17a)$$

$$k_{1b} = \frac{A_f}{V_f} P_f \quad (17b)$$

$$k_2 = \frac{A_s}{V_s} P_s \quad (17c)$$

It can be concluded that the resulted diffusion model is equivalent to the kinetic model of the consecutive reactions ($f \leftrightarrow m \rightarrow s$). The only difference is C_m which is simply obtained from the mass balance:

$$C_{m,t} = C_{m,0} + \frac{(C_{f,0} - C_{f,t})V_f}{V_m} + \frac{(C_{s,0} - C_{s,t})V_s}{V_m} \quad (18)$$

For cases, where leakage between feed and strip compartments is probable, Eqs. (16a) and (16b) were modified by taking into account the diffusion and convection mechanism of Pb transport due to leakage:

$$J_{\text{leak}} = P_{\text{leak}} (C_f - C_s) + \frac{1}{2} (C_f + C_s) J_{v,\text{leak}} \quad (19)$$

In equation (19), $J_{v,\text{leak}}$ is the volume flow due to leakage. Then the time derivative of the feed and strip concentrations become:

$$\left(\frac{dC_f}{dt}\right)_{\text{leak}} = \frac{A_{\text{leak}} J_{\text{leak}}}{V_f} = -k_{\text{leak},f} C_f + k_{\text{leak},b} C_s \quad (20a)$$

$$\left(\frac{dC_s}{dt}\right)_{\text{leak}} = -\frac{A_{\text{leak}}J_{\text{leak}}}{V_s} = k_{\text{leak},f}\frac{V_f}{V_s}C_f - k_{\text{leak},b}\frac{V_f}{V_s}C_s \quad (20b)$$

where $k_{\text{leak},f}$ and $k_{\text{leak},b}$ are defined as:

$$k_{\text{leak},f} = A_{\text{leak}} \left(\frac{P_{\text{leak}} + J_{v,\text{leak}}}{2} \right) \quad (21a)$$

$$k_{\text{leak},b} = A_{\text{leak}} \left(\frac{P_{\text{leak}} - J_{v,\text{leak}}}{2} \right) \quad (21b)$$

From Eqs. (16a), (16b), (18), (20a), and (20b) we get:

$$\frac{dC_f}{dt} = a_0C_{f,0} + a_fC_f + a_sC_s \quad (22a)$$

$$\frac{dC_s}{dt} = b_0C_{f,0} + b_fC_f + b_sC_s \quad (22b)$$

The meaning of the parameters a_i , b_i ($i = 0, f, s$) and the solution of Eqs. (22a) and (22b) for the condition $C_{m,0} = C_{s,0} = 0$ is as follows:

$$a_0 = \frac{A_f P_f}{V_m} \quad (23a)$$

$$a_f = \frac{(A_f P_f K_{p,f} + k_{\text{leak},1})}{V_f + a_0} \quad (23b)$$

$$a_s = \frac{(k_{\text{leak},2} - a_0 V_s)}{V_f} \quad (23c)$$

$$b_0 = \frac{A_s P_s V_f}{(V_m V_s)} \quad (24a)$$

$$b_f = \frac{k_{\text{leak},1}}{V_s - b_0} \quad (24b)$$

$$b_s = \frac{A_s P_s}{V_m} + \frac{k_{\text{leak},2}}{V_s} \quad (24c)$$

$$\frac{C_f}{C_{f,0}} = \frac{1}{2d} \left[\frac{2(a_0 b_s + a_s b_0) + \left(\frac{g_1}{r} - g_2\right) \exp\left(-\frac{(r+a_f+b_s)t}{2}\right) - \left(\frac{g_1}{r} + g_2\right) \exp\left(\frac{(r-a_f-b_s)t}{2}\right)}{\left(\frac{g_1}{r} + g_2\right) \exp\left(\frac{(r-a_f-b_s)t}{2}\right)} \right] \quad (25a)$$

$$\frac{C_s}{C_{f,0}} = \frac{1}{2d} \left[\frac{2h_1 + \left(\frac{h_2}{r} - h_1\right) \exp\left(-\frac{(r+a_f+b_s)t}{2}\right) - \left(\frac{h_2}{r} + h_1\right) \exp\left(\frac{(r-a_f-b_s)t}{2}\right)}{\left(\frac{h_2}{r} + h_1\right) \exp\left(\frac{(r-a_f-b_s)t}{2}\right)} \right] \quad (25b)$$

where

$$d = a_f b_s - a_s b_f \quad (26a)$$

$$g_1 = a_0 (2a_s b_f + b_s^2) + a_f a_s (b_0 - b_f) + b_s (a_s (b_0 + b_f) + a_f (a_f - a_0 - b_s)) \quad (26b)$$

$$g_2 = a_f (b_0 + b_f) + a_0 b_s - a_f b_s \quad (26c)$$

$$h_1 = a_f b_0 + a_0 b_f \quad (26d)$$

$$h_2 = a_f (b_0 (a_f - b_s) + a_0 b_f - 2b_f b_s) + b_f (2a_s (b_0 + b_f) + a_0 b_s) \quad (26e)$$

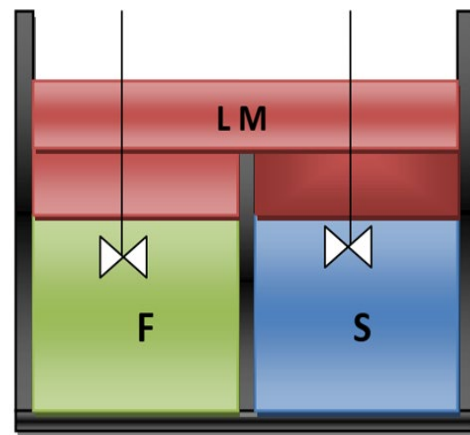
$$r = (a_f^2 + 4a_s b_f - 2a_f b_s + b_s^2) \quad (26f)$$

There are five model parameters (P_f , $K_{p,f}$, P_s , $k_{\text{leak},f}$, $k_{\text{leak},b}$) to be fitted. For simplicity and to reduce this number, it was assumed that $P_f = P_s$ and the model parameters were obtained by minimizing the sum of squared errors of prediction, sum of squared estimate (SSE):

$$\text{SSE} = \sum_i \frac{\left((C_{f,\text{mod},i} - C_{f,\text{exp},i})^2 + (C_{s,\text{mod},i} - C_{s,\text{exp},i})^2 \right)}{C_{f,\text{exp},0}^2} \quad (27)$$

3. Experimental work

Fig. 2 demonstrates the setup used to carry out experiments for model validation. It consists of a rectangular glass vessel (80 mm height \times 180 mm length \times 60 mm width) divided into two compartments by a 60 mm-height glass plate of 2 mm thickness. One compartment was filled with an aqueous feed (F) phase and the other with an aqueous strip (S) phase. The two aqueous phases were layered with a liquid membrane (LM) phase above them. The glass plate



F: Feed phase, S: Strip Phase, LM: Liquid Membrane

Fig. 2. Schematic diagram of bulk liquid membrane setup.

was placed at specific positions so that it gives ($V_s:V_f$) volume ratios of 1:1, 1:2, and 2:1. For those ratios the contact area feed-LM and strip-LM were; $A_f = 54, 72, 36 \text{ cm}^2$, $A_s = 54, 36$, and 72 cm^2 , respectively. The volumes of feed and strip were $V_f = 300, 410$, and 205 cm^3 and $V_s = 300, 205$, and 410 cm^3 , respectively; the LM volume was $V_m = 108 \text{ cm}^3$.

All experiments were carried out at room temperature of $23^\circ\text{C} \pm 2^\circ\text{C}$. Mechanical mixers were used to continuously stir feed and strip phases to reduce both boundary layers (feed-side and strip-side boundary layers). The mixing speed was set at $200 \pm 10 \text{ rpm}$. Aqueous feed phase was prepared in a beaker of 500 mL, by dissolving $\text{Pb}(\text{CH}_3\text{COO})_2$ in distilled water and adjusted by adding drops of 1 M hydrochloric acid until the required pH is attained. Also, the aqueous strip phase was simply prepared as distilled water adjusted with 0.2 N NaOH, and then EDTA was added as a stripping agent. The membrane phase was simply prepared by taking 250 mL kerosene and adding (2.5%–12.5% v/v) TBP as a carrier. Samples of each phase were collected at regular time intervals of 1 h each, while each experiment lasted for 5 h. Then, a flame atomic absorption spectrophotometer was used to measure the Pb(II) concentration for each sample. The experimental conditions of each run are shown in Table 1.

4. Results and discussions

The model was tested under two conditions; non-leakage and probable leakage conditions. Leakage may happen through the partitioning plate. Fig. 3 compares both non-leakage and probable leakage model results with experimental results under run1 conditions. The comparison clearly shows that a probable leakage exists as experimental (dispersed points) and model (solid lines) results are comparable. To precisely predict the model parameters, the equality of permeability coefficients on both sides of the liquid membrane ($P_f = P_s = P$) was assumed; thus the number of experimental points exceeded the number of model parameters. The optimal model parameters are shown in Table 2. For the volume ratio ($V_s:V_f = 1:2$), the model fittings of experimental results are shown in Figs. 3 and 4. The fitting of experimental points for ($V_s:V_f = 2:1$) failed. It yielded too low values of partition coefficient, $K_{p,f}$ and high values of permeability coefficient, P . Therefore, these experimental data were excluded from the further discussions.

Regarding $V_s:V_f = 1:1$ and 1:2, the values of P are within the range 0.8–3, which seems to be a reasonable range. Assuming that the diffusion coefficient is of the order $10^{-5} \text{ cm}^2/\text{s}$, the thickness of the diffusion boundary layers is 10^{-2} cm and $K_p \approx 1$, and the value of P is around 2 cm/h. The difference between P for $V_s:V_f = 1:1$ (ca. 3 cm/h) and for 1:2 (ca. 0.8 cm/h) is probably caused by different stirring. The discrepancy of the values of partition coefficient, $K_{p,f}$ from run to run is 0.5–1.6 and the average value of $K_{p,f}$ may be considered equal to 1.

In Figs. 5 and 6, the time dependence of (C/C_0) for both experimental results and model fitting is compared. It is seen that for $V_s:V_f = 1:2$ (Fig. 5), a good agreement was obtained, while $V_s:V_f = 2:1$ (Fig. 6) a considerable discrepancy between experimental and model results is observed.

In Fig. 7, the experimental feed, strip, and membrane concentration profiles at two solute feed concentrations

Table 1
Experimental conditions

Run	$V_s:V_f$	Initial Pb(II) conc. (ppm)	Feed pH	Strip pH	Carrier (v/v)%	EDTA conc. (M)
1	1:1	50	5	2	12.5	0.1
2	1:1	50	5	2	12.5	0.01
3	1:1	50	5	12	12.5	0.1
4	1:2	50	4	8	12.5	0.1
5	1:2	50	4	9	12.5	0.01
6	1:2	50	4	8	12.5	0.1
7	2:1	100	5	11	12.5	0.1
8	2:1	100	6.5	11	12.5	0.01
9	2:1	100	6.5	11	12.5	0.1

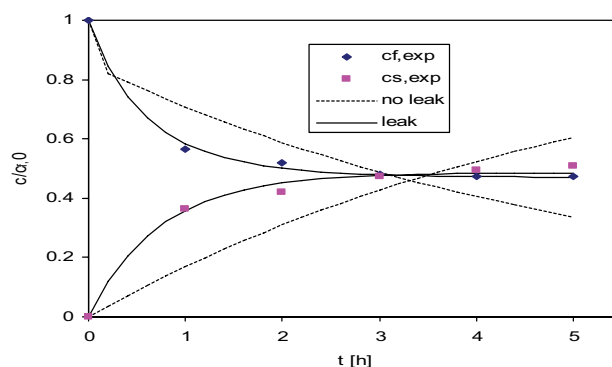


Fig. 3. Comparison of model variants: without leakage (dash line) and with leakage (solid line); run 1.

Table 2
Model parameters under leakage conditions ($k_{\text{leak},f}$ and $k_{\text{leak},b}$)

$V_s:V_f$	Run	SSE	P (cm/h)	$K_{p,f}$	$k_{\text{leak},f}$ (1/h)	$k_{\text{leak},b}$ (1/h)
1:1	1	0.011	3.25	0.84	0.31	0.54
	2	0.0029	3.25	0.49	0.59	0.72
	3	0.0068	1.81	1.64	3.6×10^{-9}	0.08
1:2	1,2	0.018	3.22	0.65	0.45	0.62
	4	0.0052	0.84	1.48	0.42	0.51
	5	0.0076	0.83	1.25	0.34	0.37
	6	0.0043	0.70	0.47	0.27	0.26
4–6	4–6	0.047	0.80	1.05	0.33	0.37
	7	0.076	135	2×10^{-10}	0.96	0.85
	2:1	8	0.086	304	9×10^{-11}	0.82
2:1	9	0.15	1×10^6	3×10^{-7}	0.59	0.50
	7–9	0.32	49	5×10^{-10}	0.77	0.66

(25 and 200 ppm) are shown. When higher solute concentration (200 ppm) was investigated, accumulated solute concentration within the membrane phase was realized and the interpretation of that could be due to higher transport rate and saturation limits of membrane phase. This has led to the conclusion of less extraction efficiency may be obtained. A comparison between theoretical and experimental trends

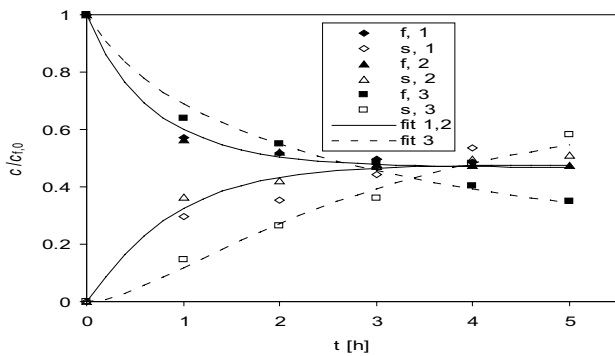


Fig. 4. Dependence of C/C_{f0} on time – comparison of the experimental data and their model fitting for runs 1–3 ($V_s:V_f = 1:1$); f : feed, s : strip, solid line: fit of runs 1 and 2 ($\text{pH}_{\text{strip}} = 2$), dash line: fit of run 3 ($\text{pH}_{\text{strip}} = 12$).

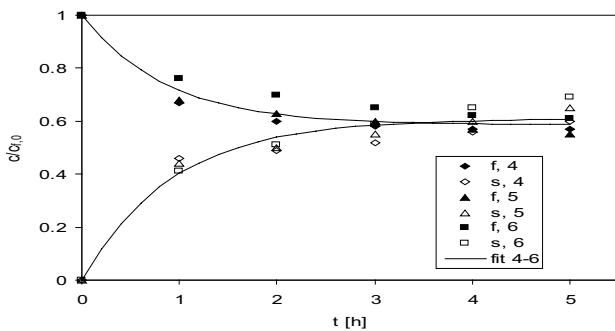


Fig. 5. Dependence of C/C_{f0} on time – comparison of the experimental data and their model fitting for runs 4–6 ($V_s:V_f = 1:2$); f : feed, s : strip.

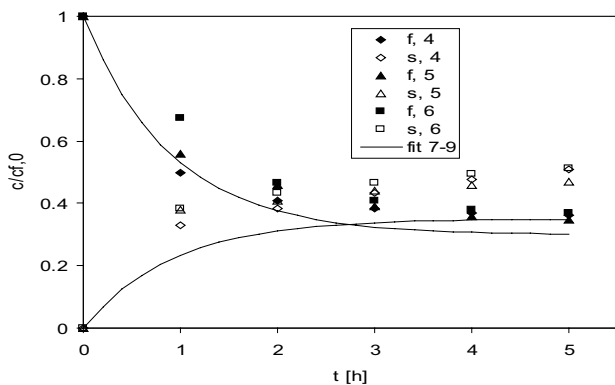


Fig. 6. Dependence of C/C_{f0} on time – comparison of the experimental data and their model fitting for runs 7–9 ($V_s:V_f = 2:1$); f : feed, s : strip.

of concentration profiles shows a significant difference in the effect of initial feed concentration on the extraction efficiency of Pb^{2+} ions between theoretical and experimental results. The theoretical results tend to be insensitive to the effect of initial feed concentration, and the reason behind that is the non-inclusion of initial concentration in the model. The model

is mainly dependent on feed, strip, and membrane volumes, which are indirectly reflected as solute concentration.

Although the effect of the pH of feed and strip phases on the transport kinetics was considered indirectly represented through the variation of the transport rate constants (k_1 and k_2), experimental investigations of the effect of pH on both extraction and stripping efficiencies were conducted and demonstrated in Figs. 8 and 9.

Fig. 8 shows that the pH of the feed phase has a direct impact on feed concentration profiles at pH values; 2, 3, 4, and 5. The extraction efficiency was found to increase as the feed pH increase from the value 2 to 5. The initial transport rate of the solute from the feed phase is also directly proportional to the value of the pH. Similarly, Fig. 9 shows that high acidity of the strip phase solution results in higher extraction and stripping efficiencies. However, the alkalinity of the strip phase solution was also investigated and shown in Fig. 10. It was found that high alkalinity also exhibits high extraction and stripping efficiencies.

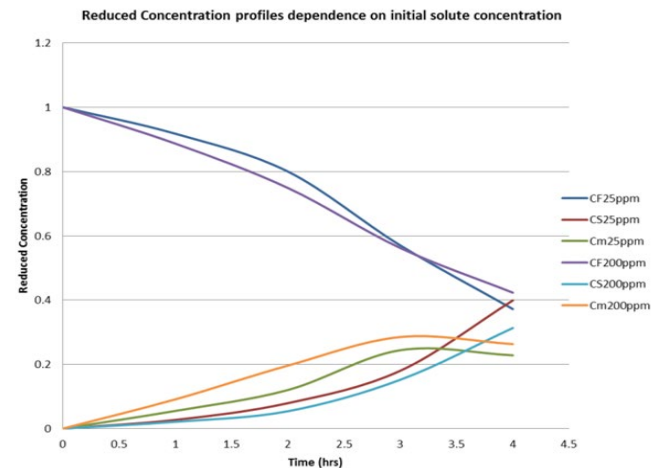


Fig. 7. Feed, strip, membrane experimental reduced concentration (C/C_0) profiles at two solute concentrations (25 and 200 ppm) and $S:F = 2:1$.

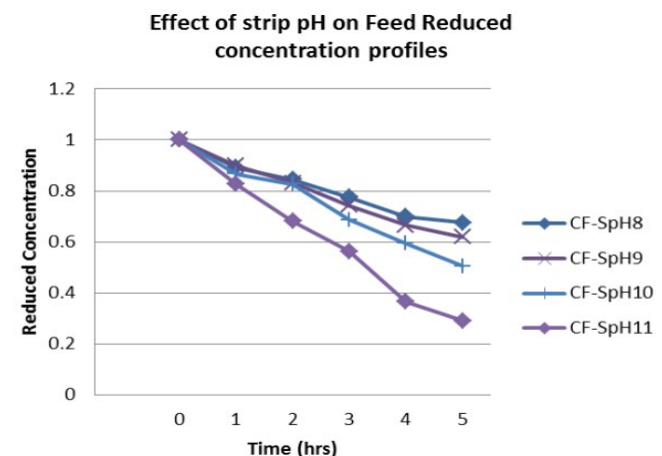


Fig. 8. Effect of feed pH on feed reduced concentration (C/C_0) profiles at $V_s:V_f = 1:1$ and initial solute concentration (50 ppm).

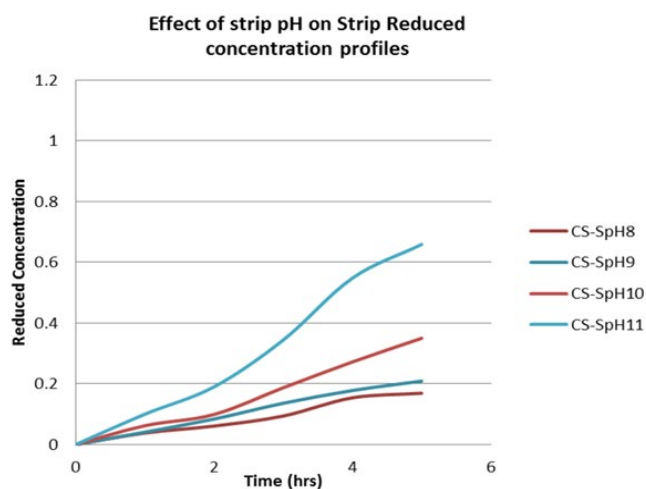


Fig. 9. Effect of strip pH on strip reduced concentration (C/C_0) profiles at $V_s:V_f = 1:1$ and initial solute concentration (50 ppm).

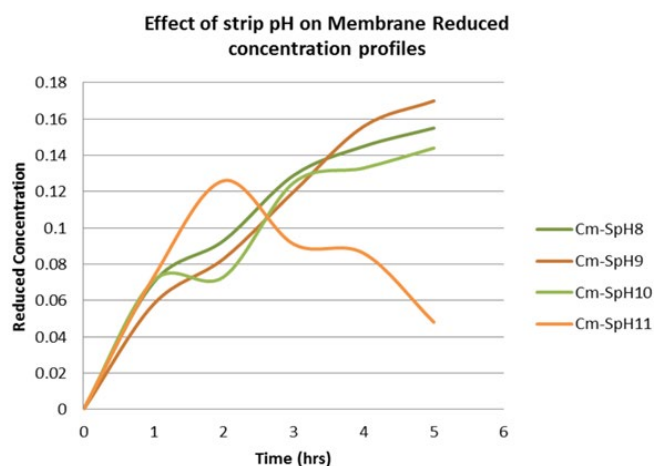


Fig. 10. Effect of strip pH on membrane reduced concentration (C/C_0) profiles at $V_s:V_f = 1:1$ and initial solute concentration (50 ppm).

Fig. 10 shows considerable extraction and stripping efficiencies at (pH = 11), and both concentration profiles tend to maximum trend and slope. It was found that the high alkalinity of the strip phase results in better performance of liquid membrane performance to extract Pb^{2+} ions. This leads to operating liquid membrane systems at a high pH gradient between feed and strip phases. The high pH gradient is considered a major driving force for the transport of metal ions across the membrane phase. It was found that feed pH of 5 and strip pH of 11 contributed to high selectivity of Pb^{2+} ions extraction and transport.

5. Conclusions

A comparison between theoretical and experimental results of Pb^{2+} removal from aqueous solutions using liquid membrane processes was carried out and revealed that manipulating the operating conditions of the process will

significantly affect the removal efficiency. The prediction of Pb^{2+} removal and concentration profiles were attempted using simple diffusive transport models. The comparison of the theoretical and experimental results has shown that fair agreement was accomplished. It was shown that both experimental and theoretical results have the same trend of profile. The inclusion of the effect of carriers added to the membrane phase on the model accuracy was found to be important. Higher partition coefficients resulted in higher accumulation of lead ions within the membrane phase and consequently imposes a higher driving force to accelerate the transport of lead ions towards the stripping phase.

TBP was found to be an effective carrier to facilitate the lead ions transport and increase removal efficiency. Up to 95% removal efficiency was obtained under certain conditions. When a blank experiment (no carrier) was carried out, no Pb^{2+} ions transport was detected, suggesting that the transport of Pb^{2+} through membranes depends on the complexation and de-complexation mechanism of TBP- Pb^{2+} . Various TBP concentrations (2.5%, 5%, 7.5%, 10%, and 12.5% (v/v)) in kerosene membrane were studied to investigate its effect on the transport efficiency of lead at ambient temperature ($23^\circ\text{C} \pm 2^\circ\text{C}$) and mixing speed of 200 ± 10 rpm.

References

- [1] S.Y. Kazemi, M. Shamsipur, Selective transport of lead(II) through a bulk liquid membrane using a cooperative carrier composed of benzylaza-12-crown-4 and oleic acid, *Bull. Korean Chem. Soc.*, 26 (2005) 930–934.
- [2] S. Khaoya, U. Pancharoen, Removal of lead(II) from battery industry wastewater by HFSLM, *Int. J. Chem. Eng. Appl.*, 3 (2012) 98–103.
- [3] M.A. Akl, An improved colorimetric determination of lead (II) in the presence of nonionic surfactant, *Anal. Sci.*, 22 (2006) 1227–1231.
- [4] V. Inglezakis, H. Grigoropoulou, Modeling of ion exchange of Pb^{2+} in fixed beds of clinoptilolite, *Microporous Mesoporous Mater.*, 61 (2003) 3079–3086.
- [5] K. Kavallieratos, J.M. Rosenberg, W.Z. Chen, T. Ren, Fluorescent sensing and selective Pb(II) extraction by a dansylamide ion exchange, *J. Am. Chem. Soc.*, 127 (2005) 6514–6515.
- [6] B. Menoyo, M.P. Elizalde, A. Almela, Extraction of lead by cyanex 302 from phosphoric acid media, *Solvent Extr. Ion Exch.*, 19 (2001) 677–698.
- [7] T.N. Shilimkar, M.A. Anuse, Rapid extraction of lead (II) from succinate media with n-octylaniline in toluene, *Sep. Purif. Technol.*, 26 (2002) 185–193.
- [8] J.L. Manzoori, H.A. Zadeh, Extraction and preconcentration of lead using cloud point methodology: application to its determination in real samples by flame atomic absorption spectrometry, *Acta Chim. Solv.*, 54 (2007) 378–384.
- [9] M. Ghaedi, A. Shokrollahi, K. Niknam, E. Niknam, A. Najibi, M. Soylak, Cloud point extraction and flame atomic absorption spectrometric determination of cadmium(II), lead(II), palladium(II) and silver(I) in environmental samples, *J. Hazard. Mater.*, 168 (2009) 1022–1027.
- [10] S.K. Singh, S.K. Misra, S.C. Tripathi, D.K. Singh, Studies on permeation of uranium(VI) from phosphoric acid medium through supported liquid membrane comprising a binary mixture of PC88A and Cyanex 923 in n-dodecane as carrier, *Desalination*, 250 (2010) 19–25.
- [11] B. Tang, G. Yu, J. Fang, T. Shi, Recovery of high purity silver directly from dilute effluents by an emulsion liquid membrane-crystallization process, *J. Hazard. Mater.*, 177 (2010) 377–383.
- [12] V.S. Kislik, *Liquid Membranes: Principles and Applications in Chemical Separations and Wastewater Treatment*, 1st ed., Elsevier B.V., 2010.

- [13] P.R. Danesi, C. Cianetti, Multistage separation of metal ions with a series of composite supported liquid membranes, *J. Membr. Sci.*, 20 (1984) 215–226.
- [14] A.O. Saf, S. Alpaydin, A. Sirit, Transport kinetics of chromium(VI) ions through a bulk liquid membrane containing p-tert-butyl calix[4]arene 3-morpholino propyl diamide derivative, *J. Membr. Sci.*, 283 (2006) 448–455.
- [15] W. Zhang, J. Liu, Z. Ren, S. Wang, C. Du, J. Ma, Kinetic study of chromium(VI) facilitated transport through a bulk liquid membrane using tri-n-butyl phosphate as carrier, *Chem. Eng. J.*, 150 (2009) 83–89.
- [16] M. Ma, D. He, Q. Wang, Q. Xie, Kinetics of europium (III) transport through a liquid membrane containing HEH (EHP) in kerosene, *Talanta*, 55 (2001) 1109–1117.
- [17] H.K. Alpoguz, S. Memon, M. Ersoz, M. Yilmaz, Transport of Hg^{2+} through bulk liquid membrane using a bis-calix[4]arene nitrile derivative as carrier: kinetic analysis, *New J. Chem.*, 26 (2002) 477–480.
- [18] S. Koter, P. Szczepanski, M. Mateescu, G. Nechifor, L. Badalau, I. Koter, Modeling of the cadmium transport through a bulk liquid membrane, *Sep. Purif. Technol.*, 107 (2013) 135–143.
- [19] E.A. Burns, D.N. Hume, Acetato complexes of lead in aqueous solution, *J. Am. Chem. Soc.*, 78 (1956) 3958–3962.
- [20] A. Kargari, S. Mohammadi, T. Kaghazchi, A model for metal ion pertraction through supported liquid membranes, *Desalination*, 219 (2008) 324–334.
- [21] T. Sadyrbaeva, Liquid membrane system for extraction and electrodeposition of lead (II) during electro dialysis, *Mater. Sci. Appl. Chem.*, 34 (2017) 29–33.
- [22] O. Durmaz, R. Donat, H. Cetişli, Transportation of Pb(II) ions with D2EHPA as carrier by MDLM system, *Int. J. Innovative Res. Sci. Eng. Technol.*, 5 (2016) 48–56.
- [23] N. El-Said, N. Abdel Rahman, M.M.S. Ali, Carrier mediated transport of toxic elements, Part II Transport modeling for extraction of Pb (II) by Cyanex302/xylene as carrier from nitrate medium using SLM, *J. Appl. Chem.*, 7 (2014) 85–92.
- [24] O. Arous, F.S. Saoud, M. Amara, H. Kerdjoudj, Efficient facilitated transport of lead and cadmium across a plasticized triacetate membrane mediated by D2EHPA and TOPO, *Mater. Sci. Appl.*, 2 (2011) 615–623.
- [25] L. Pei, L.-m. Wang, Transport behavior of divalent lead ions through disphase supplying supported liquid membrane with PC-88A as mobile carrier, *Int. J. Chem. Reactor Eng.*, 10 (2012) 1–24.
- [26] K. Makino, H. Ohshima, T. Kondo, Kinetic model for membrane transport; 1. Effects of membrane volume and partitioning kinetics, *Biophys. Chem.*, 35 (1989) 85–95.